Available online at www.sciencedirect.com
ScienceDirect
Journal of Sound and Vibration 299 (2007) 884–899
JOURNAL OF SOUND AND VIBRATION
www.elsevier.com/locate/jsvi

Identification of rigid body properties from vibration measurements

R.A.B. Almeida[a], A.P.V. Urgueira[a], N.M.M. Maia[b,*]

[a]*Department Engenharia Mecânica e Industrial, Faculdade de Ciências e Tecnologia, 2829-516 Monte de Caparica, Portugal*
[b]*Department Eng. Mec., Instituto Superior Técnico, Av. Rovisco Pais, 1049-001 Lisboa, Portugal*

Received 30 March 2005; received in revised form 13 June 2006; accepted 19 July 2006

Abstract

A knowledge of the rigid body properties of a structure can be important in vibration analysis, control, optimisation and structural dynamic problems in general. Whenever a system has a complicated shape and the location of its centre of mass and inertia tensor cannot be easily determined by purely theoretical tools, it may be convenient to use measured experimental dynamic data and to apply appropriate methods to evaluate those properties.

In the present work a parametric modal identification method is investigated, for the simultaneous estimation of all the rigid body properties, using information from measured Frequency Response Functions encompassing the low-frequency modes. An important numerical tool has been developed to act as an indicator factor for mode shape selection, which can help to build the best available modal matrix. The accuracy of the estimated parameters is evaluated through the application of the method to a theoretical example, as well as to an actual structure specifically designed and built for this purpose.

Keywords: Rigid body; Identification; Modal analysis

1. Introduction

The evaluation of the rigid body properties of a structure (mass, centre of mass location and inertia tensor) is a very important task during a static or dynamic design process. These properties can be estimated using analytical approaches, such as solid or finite element modelling. In fact, when a model of the structure, exists from the initial design process, very little additional time is required to obtain the inertia properties. If such a model does not exist, or when modifications are made to the original structure the establishment of an accurate model can be very time consuming. The alternative may reside on the use of experimental data readily available from measurements.

This problem has been addressed by various authors [1–5] that have developed dynamic methods for the identification of rigid body properties; those methods may be separated into two main

*Corresponding author. Tel.: +351 218417454; fax: +351 218417915.
E-mail address: nmaia@dem.ist.utl.pt (N.M.M. Maia).

0022-460X/$ - see front matter © 2006 Elsevier Ltd. All rights reserved.
doi:10.1016/j.jsv.2006.07.043

categories:

- Time domain methods;
- Frequency domain methods.

The early Time domain methods to mention are the classical pendulum methods, which can effectively determine some rigid body parameters and are still in use [6], but for complex structures such an estimation may not be that easy. For instance, the pendulum test requires special skills and is prone to large experimental errors. More recently, some authors developed other variations for the Time domain methods, like Pandit [7], who presents a systematic way to calculate the rigid body characteristics through a careful selection of rigid body modes and mode shapes obtained from time domain impact data. All of the parameters are determined by solving simultaneous linear equations. Hahn [8] uses the time domain test data of a six-axes shaking table system where the exciter forces are measured in addition to the acceleration responses. The advantage of these methods is the direct evaluation of the test data without transforming it into the frequency domain. A disadvantage is that if the system under observation does not behave like a rigid body in the excited frequency range, low pass filtering of the test data must be performed.

Frequency domain methods can circumvent this drawback because it is possible to separate the rigid and elastic system behaviour, even if the first elastic natural frequency is very low. The Frequency domain methods can be divided into three groups:

- Inertia Restraint Methods (IRM);
- Methods of Direct Physical Parameter Identification (MDPPI);
- Modal Methods (MM).

The Inertia Restraint Methods or Mass Line Methods have been widely studied and they stand on the principle that the dynamic response of freely supported structures is characterized, in the low-frequency region, by a constant term designated as ''inertia restraint'' or ''mass line''. They are suitable for the cases where the rigid and flexible modes are well separated. Some investigators have explained how to determine the mass line of a typical Frequency Response Function (FRF) of a free–free structure, as it can be found in the works of Ewins [9], Lamontia [10], Crowley [11] and Tominaga [12]. These methods can be grouped into: iterative and direct methods, according to the way the inertia properties are obtained, either assuming the knowledge of one or several properties, and by an iterative process calculating the remainders, or by using directly and solely the data extracted from measured FRFs. Among the researchers that have made use of iterative methods, one can distinguish Okubo and Furukawa [13], Wei and Reis [14], Furukawa [15] and Okuzumi [16]. Concerning the direct processes one can refer the works of Bretl and Conti [17], Fregolent [18,19], and more recently Lee et al. [20], Urgueira and Almeida [21] and Almeida [29].

The Direct Physical Parameter Identification Methods allow for the determination of mass, stiffness and damping parameters through the direct use of measured FRFs. Johnson and Snyder [22], Mangus and Passarelo [23] and Huang [24,25] are amongst those who have developed these kinds of methods.

The Modal Methods are based upon the orthogonality relationship between the mass matrix and the rigid body modes. This class of methods is particularly appropriate whenever the rigid body and the flexible modes are not well separated, as it is also required by the MDPPI methods. Generally the experimental data are available from tests undertaken on ''quasi-free'' or ''softly'' suspended structures. A modal identification procedure is subsequently required to extract all the modal properties of the available rigid body modes. The main difficulty associated with these methods is that, in general, not all the rigid body modes can be simultaneously excited during an experimental test.

2. Theoretical background of modal methods

In the present work the determination of the ten inertia parameters follows closely the methodology adopted in the works of Bretl and Conti [17,26] and Toivola and Nuutila [27]. These methods make use of measured responses due to the excitation applied in various points and directions. These methods require as

many exciter locations/directions as needed to significantly excite all the six rigid body modes. In theory one excitation may be enough, in contrast with the minimum three excitations required by the IRM methods [20,29].

The FRFs measured at the response points for each excitation condition are then used to extract the modal properties (natural frequencies, damping ratios and mode shapes), using well-established identification methods [28]. If the origin of the physical coordinate system is established as a reference, the orthogonality property for mass-normalised mode shapes can be expressed as

$$\boldsymbol{\Phi}_0^{\mathrm{T}}\mathbf{M}_0\boldsymbol{\Phi}_0 = \mathbf{I}, \tag{1}$$

where $\mathbf{M}_0$ and $\boldsymbol{\Phi}_0$ represent, respectively, the 6×6 mass matrix and the 6×6 mass-normalised mode shape matrix with respect to the origin.

The first three rows of $\boldsymbol{\Phi}_0$ are associated to the translational motion whereas the last three rows are associated to the rigid body rotations of the test article. The mass matrix $\mathbf{M}_0$ can be obtained as

$$\mathbf{M}_0 = \boldsymbol{\Phi}_0^{-\mathrm{T}}\boldsymbol{\Phi}_0^{-1}. \tag{2}$$

The 6×6 mode shape matrix $\boldsymbol{\Phi}_0$ is an invertible matrix, since the six rigid mode shapes are linearly independent vectors. However, from the identification process applied to the measured FRFs, one obtains the mode shape matrix with respect to the physical coordinate system where the measurements are taken, i.e., $\boldsymbol{\Phi}$ rather than $\boldsymbol{\Phi}_0$. The relationship between both matrices is given by

$$\underbrace{\begin{bmatrix} \begin{Bmatrix}\phi_x\\ \phi_y\\ \phi_z\end{Bmatrix}_1 \\ \vdots \\ \begin{Bmatrix}\phi_x\\ \phi_y\\ \phi_z\end{Bmatrix}_N \end{bmatrix}_1 \quad \begin{bmatrix} \begin{Bmatrix}\phi_x\\ \phi_y\\ \phi_z\end{Bmatrix}_1 \\ \vdots \\ \begin{Bmatrix}\phi_x\\ \phi_y\\ \phi_z\end{Bmatrix}_N \end{bmatrix}_2 \quad \cdots \quad \begin{bmatrix} \begin{Bmatrix}\phi_x\\ \phi_y\\ \phi_z\end{Bmatrix}_1 \\ \vdots \\ \begin{Bmatrix}\phi_x\\ \phi_y\\ \phi_z\end{Bmatrix}_N \end{bmatrix}_6}_{(3N\times 6)} = \underbrace{\begin{bmatrix} \begin{bmatrix}1&0&0&0&z_1&-y_1\\0&1&0&-z_1&0&x_1\\0&0&1&y_1&-x_1&0\end{bmatrix} \\ \vdots \\ \begin{bmatrix}1&0&0&0&z_N&-y_N\\0&1&0&-z_N&0&x_N\\0&0&1&y_N&-x_N&0\end{bmatrix} \end{bmatrix}}_{(3N\times 6)} \underbrace{\begin{bmatrix} \begin{Bmatrix}\phi_{0_x}\\ \phi_{0_y}\\ \phi_{0_z}\\ \phi_{0\theta_x}\\ \phi_{0\theta_y}\\ \phi_{0\theta_z}\end{Bmatrix}_1 & \begin{Bmatrix}\phi_{0_x}\\ \phi_{0_y}\\ \phi_{0_z}\\ \phi_{0\theta_x}\\ \phi_{0\theta_y}\\ \phi_{0\theta_z}\end{Bmatrix}_2 & \cdots & \begin{Bmatrix}\phi_{0_x}\\ \phi_{0_y}\\ \phi_{0_z}\\ \phi_{0\theta_x}\\ \phi_{0\theta_y}\\ \phi_{0\theta_z}\end{Bmatrix}_6 \end{bmatrix}}_{(6\times 6)} \tag{3}$$

or simply

$$\boldsymbol{\Phi} = \mathbf{R}_0\boldsymbol{\Phi}_0, \tag{4}$$

where $\mathbf{R}_0$ represents the transformation matrix of the rigid body modes related to the N triaxial accelerometers. Generally, the resulting over-determined linear system of equations can be solved in a least-squares sense:

$$\boldsymbol{\Phi}_0 = (\mathbf{R}_0^{\mathrm{T}}\mathbf{R}_0)^{-1}\mathbf{R}_0^{\mathrm{T}}\boldsymbol{\Phi}. \tag{5}$$

Numerically we may be tempted to conclude that $\boldsymbol{\Phi}_0$ can be obtained if $\mathbf{R}_0$ contains at least data from two triaxial measurement points. However, Lee et al. [20] proved that a minimum of three triaxial measurement points are needed to evaluate $(\mathbf{R}_0^{\mathrm{T}}\mathbf{R}_0)^{-1}$. In the present paper, we have carried out several measurements with different locations for the triaxial accelerometers; the best results were obtained when the three accelerometers formed a regular triangle, thus confirming the conclusions of Lee et al. [20].

By inverting Eq. (5) one obtains $\boldsymbol{\Phi}_0^{-1}$, and using directly this result in Eq. (2) one can calculate $\mathbf{M}_0$. Therefore, the resulting matrix $\mathbf{M}_0$ represents the best least-squares mass matrix related to the origin based on

the six extracted mode shape vectors at N measured response locations and is given by

$$\mathbf{M}_0 = \left[\begin{array}{ccc:ccc} m & 0 & 0 & 0 & m\,z_{cm} & -m\,y_{cm} \\ 0 & m & 0 & -m\,z_{cm} & 0 & m\,x_{cm} \\ 0 & 0 & m & m\,y_{cm} & -m\,x_{cm} & 0 \\ \hdashline 0 & -m\,z_{cm} & m\,y_{cm} & J_{xx_0} & -J_{xy_0} & -J_{xz_0} \\ m\,z_{cm} & 0 & -m\,x_{cm} & -J_{yx_0} & J_{yy_0} & -J_{yz_0} \\ -m\,y_{cm} & m\,x_{cm} & 0 & -J_{zx_0} & -J_{zy_0} & -J_{zz_0} \end{array}\right] = \left[\begin{array}{c:c} \mathbf{M}_{\mathbf{AA}} & \mathbf{M}_{\mathbf{AB}} \\ \hdashline \mathbf{M}_{\mathbf{BA}} & \mathbf{M}_{\mathbf{BB}} \end{array}\right], \tag{6}$$

where the components of the inertia tensor are referred to the assumed original coordinates. The mass of the rigid body can be calculated as the average of the first three diagonal terms of $\mathbf{M}_0$. Equating the non-zero elements of the upper right quadrant of matrix, Eq. (6), to the same elements in mass matrix referred to the centre of mass, six equations are obtained. The estimates for the coordinates of the centre of mass are given by

$$x_{\mathrm{cm}} = \frac{1}{2m}(m_{26} - m_{35}), \quad y_{\mathrm{cm}} = \frac{1}{2m}(m_{34} - m_{16}), \quad z_{\mathrm{cm}} = \frac{1}{2m}(m_{15} - m_{24}), \tag{7}$$

where m_{ij} are the corresponding elements of the estimated mass matrix $\mathbf{M}_0$. Once the coordinates of the centre of mass have been obtained from Eq. (7), the mass matrix can be transformed into the coordinate frame that has its origin at the centre of mass by using the following transformation:

$$\mathbf{M}_{\mathbf{cm}} = \left[\begin{array}{c:c} \mathbf{I} & \mathbf{R}_{\mathbf{cm}} \\ \hdashline 0 & \mathbf{I} \end{array}\right]^{\mathrm{T}} \left[\begin{array}{c:c} \mathbf{M}_{\mathbf{AA}} & \mathbf{M}_{\mathbf{AB}} \\ \hdashline \mathbf{M}_{\mathbf{BA}} & \mathbf{M}_{\mathbf{BB}} \end{array}\right] \left[\begin{array}{c:c} \mathbf{I} & \mathbf{R}_{\mathbf{cm}} \\ \hdashline 0 & \mathbf{I} \end{array}\right] \tag{8}$$

where $\mathbf{R}_{\mathrm{cm}}$ represents the transformation matrix to the centre of mass coordinates, given by

$$\mathbf{R}_{\mathrm{cm}} = \begin{bmatrix} 0 & -z_{\mathrm{cm}} & y_{\mathrm{cm}} \\ z_{\mathrm{cm}} & 0 & -x_{\mathrm{cm}} \\ -y_{\mathrm{cm}} & x_{\mathrm{cm}} & 0 \end{bmatrix}. \tag{9}$$

As stated in works by Bretl and Conti [17,26], all the six rigid body modes must be extracted/identified prior to the estimation of the mass matrix. However, in practical set-ups there might be difficulties in exciting or identifying some of the rigid body modes. The work of Toivola and Nuutila [27] partially solves this problem as it requires only a subset of the 21 independent orthogonality conditions, or in other words it requires only four identified modes. In fact, from the orthogonality condition between two modes with respect to the mass matrix (Eq. (1)), it follows that

$$\boldsymbol{\phi}_{0i}^{\mathrm{T}} \mathbf{M}_0 \boldsymbol{\phi}_{0j} = \delta_{ij} \ \text{ with } \ \delta_{ij} = \begin{cases} 1, & i = j, \\ 0, & i \neq j. \end{cases} \tag{10}$$

Taking into account the nature of the rigid body mass matrix, it turns out that if n modes are estimated there are $n(n+1)/2$ independent equations. As ten unknowns are to be determined, Toivola and Nuutila's method [27] only requires at the least four mode shapes. If five or six modes can be estimated, the resulting set of equations can be solved in a least-squares sense. By using this method only one mass value is obtained. The components of the inertia tensor are referred to the origin of the system of coordinates and should be transformed to the centre of mass using the coordinate transformation as presented in Eq. (8).

In practical set-ups it is difficult to excite simultaneously all the six rigid body modes. If some of them are weakly excited, it could lead to erroneous estimation of the ten properties. In this work a new approach is used, where the modal matrix $\boldsymbol{\Phi}_0$ is formed with the best modes available from different excitation conditions. The election of the best modes is carried out by using a valuable indicator—the Norm Indicator (NI) [29,30]. In fact, with this indicator it is possible to select the most excited modes obtained from different sets of identified experimental modes. The best modes will form the final modal matrix $\boldsymbol{\Phi}_0$ to be used in

Eqs. (2) or (10). This indicator can be calculated as

$$\mathrm{NI}(\omega) = 20\ \log\left(\sqrt{\sum_{i=1}^{n}((\mathrm{Re}(\alpha_i(\omega)))^2 + (\mathrm{Im}(\alpha_i(\omega)))^2)}\right),$$
$$n = \text{number of FRFs}, \tag{12}$$

where Re and Im are the real and imaginary parts of the n $\alpha_i(\omega)$ FRFs related to each measuring direction versus excitation force.

This approach solves the difficulties inherent to Bretl and Conti and Toivola and Nuutila methods, as it is always possible to build a $\mathbf{\Phi}_0$ matrix containing the best modes resulting from various excitation conditions.

3. Test cases

In this paper two case studies are presented: the first is a numerical case and the second is an experimental one.

3.1. Test Case I—numerical

For the rigid body described in Fig. 1, three measurement points and five applied forces are considered. The three measurement points were selected taking into account the recommendations proposed by Lee et al. [20]. For the applied forces F_{0_x}, F_{0_y}, and F_{0_z} the suspension is performed as presented in Fig. 2—set-up A, when the suspension springs are applied in the horizontal plane passing through the centre of mass; for the forces

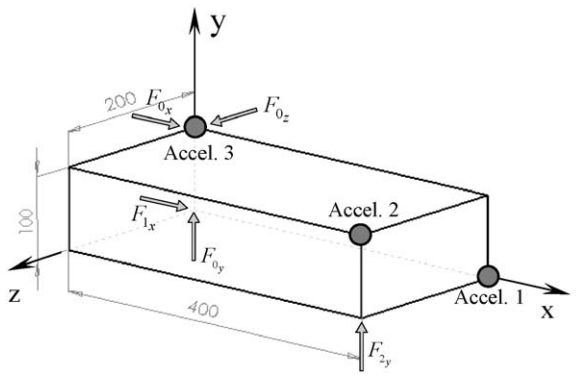

$mass = 62.8\ \mathrm{kg}$
$x_{cm} = 0.2\ \mathrm{m}$
$y_{cm} = 0.05\ \mathrm{m}$
$z_{cm} = 0.1\ \mathrm{m}$
$J_{xx\,cm} = 0.26167\ \mathrm{kg\,m^2}$
$J_{yy\,cm} = 1.04667\ \mathrm{kg\,m^2}$
$J_{zz\,cm} = 0.88967\ \mathrm{kg\,m^2}$
$J_{xy\,cm} = J_{yx\,cm} = J_{xz\,cm} = J_{zx\,cm} = J_{yz\,cm} = J_{zy\,cm} = 0\ \mathrm{kg\,m^2}$

Fig. 1. Characteristics of the rigid body in test case I.

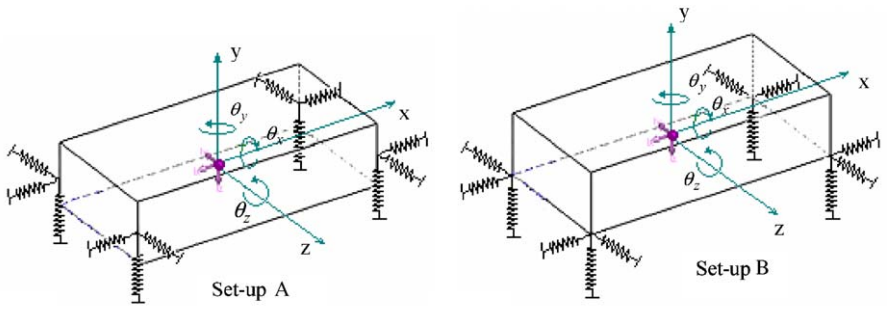

Fig. 2. Different configurations of the suspension.

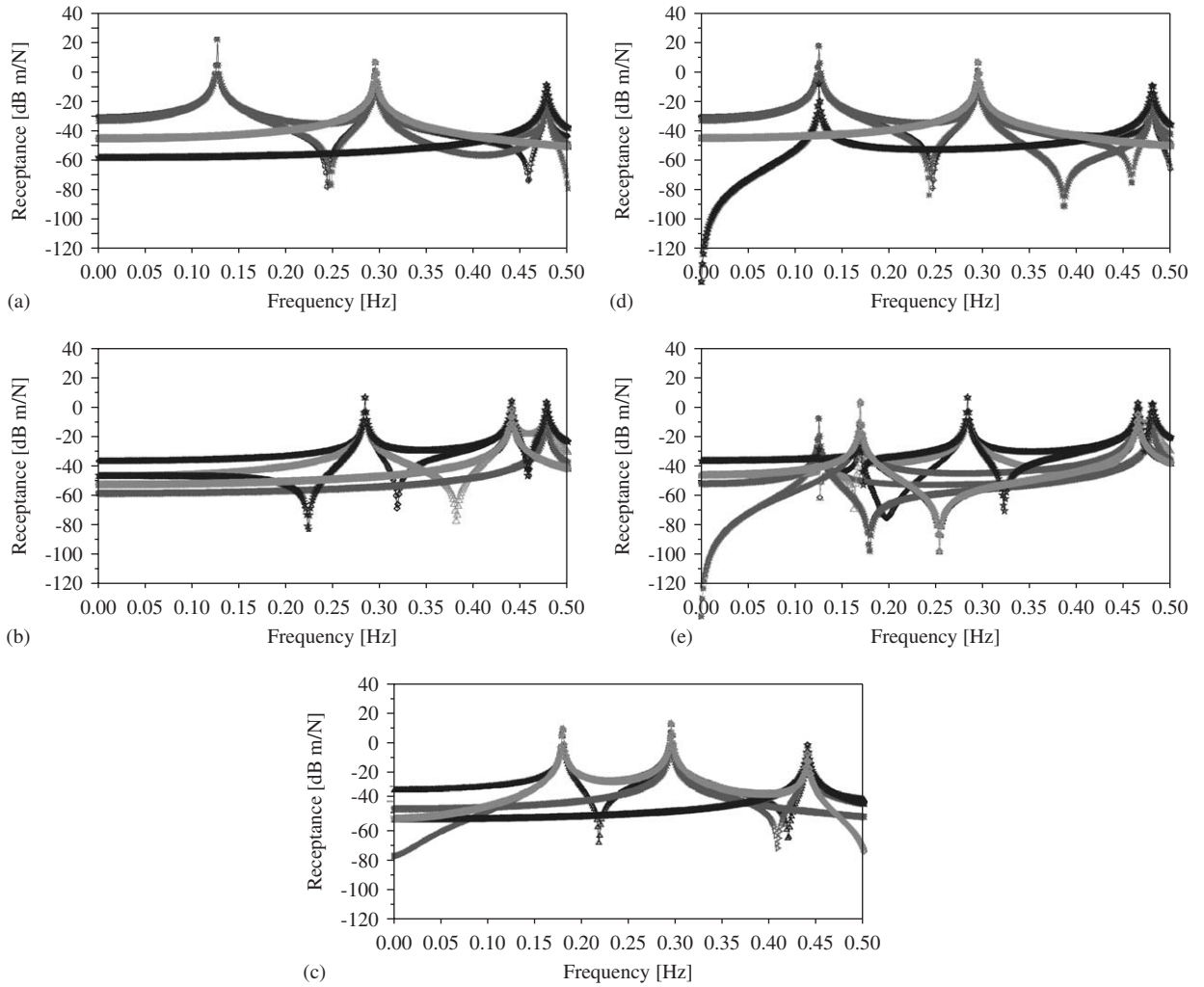

Fig. 3. Receptance FRFs obtained at each point in all three directions for each applied force in test case I (a) F_{0_x}(set-up A), (b) F_{0_y} (set-up A), (c) F_{0_z} (set-up A), (d) F_{1_x} (set-up B), (e) F_{2_y} (set-up B). —⊕—, x_1; —◇—, y_1; —△—, z_1; —✳—, x_2; —△—, y_2; —▷—, z_2; —✳—, x_3; —☆—, y_3; —◇—, z_3.

F_{1_x} and F_{2_y}, although the suspension springs are the same, these are applied in the horizontal plane parallel to the centre of mass (Fig. 2, set-up B). On each measurement point the receptance FRFs are calculated according to the three orthogonal directions x, y, z.

Low proportional damping is considered in these simulations and no artificial noise is added to the FRFs.

In this test case each spring has the following stiffness properties: $k_x = 10\,\mathrm{N\,m^{-1}}$, $k_y = 50\,\mathrm{N\,m^{-1}}$and $k_z = 20\,\mathrm{N\,m^{-1}}$.

The modulus of the receptance FRFs are presented in Fig. 3. These receptances are calculated for each applied force and three orthogonal coordinate directions.

As shown in Fig. 3, none of the applied forces could excite all of the six rigid body modes, so we have decided to use the approach presented in Section 2 to obtain the information/properties about all the rigid body modes. Specifically, it is possible to use the information of the best available rigid body modes through the NI, defined in Eq. (12). This gives us not only information about the most excited modes, but also about their level of excitation.

By observing the results obtained with the NI (Fig. 4) for the excitation forces F_{0_x}, F_{0_y} and F_{0_z} with spring suspension in set-up A, and excitation forces F_{1_x} and F_{2_y} with spring suspension in set-up B, one concludes

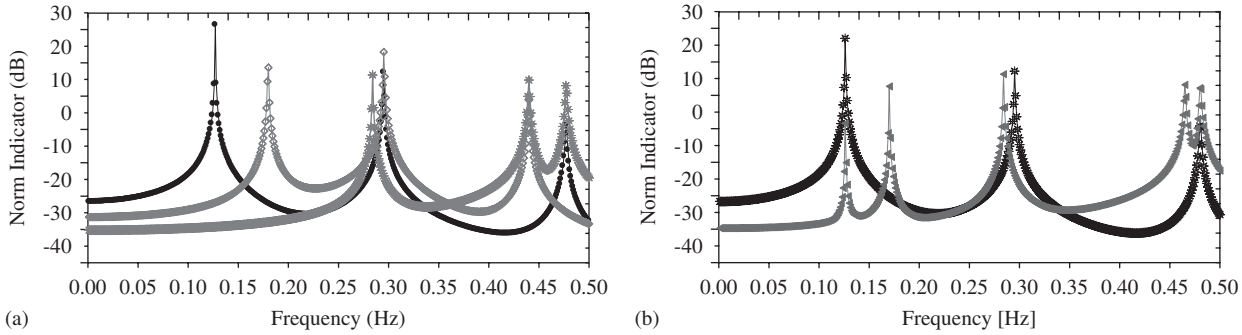

Fig. 4. Norm Indicator results with forces (a) —●—, F_{0_x}; —✳—, F_{0_y}; —◇—, F_{0_z} in set-up A and (b) —✳—, F_{1_x}; —◀—, F_{2_y} in set-up B.

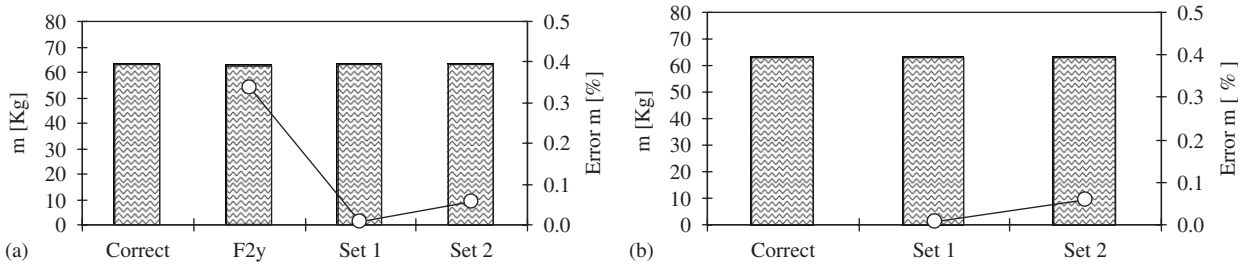

Fig. 5. Results of the mass parameter and relative error for (a) sets 1 and 2 using Bretl and Conti method and (b) for sets 1, 2 and F_{2_y} with Toivola and Nuutila method. ▨, m; –○–, error m.

that there are forces for which the rigid body modes are more excited than others or even not all of the rigid body modes are excited. In this particular case, for set-up A the force F_{0_x} excites mostly modes number 1, 4 and 6, F_{0_y} modes number 3, 5 and 6 and F_{0_z} modes number 2, 4 and 5. For set-up B, force F_{1_x} excites mostly modes number 1, 4 and 6, while F_{2_y} excites preferably modes number 1, 2, 3, 5 and 6.

For each set of nine FRFs obtained for each excitation, the necessary modal analysis is undertaken in order to obtain information about the modal parameters (natural frequency, mode shape and damping ratio). This process makes use of the modal analysis software MODENT [31], implementing a specific tool single input-multiple output (SIMO) analysis.

The results obtained from the modal analysis and from the NI for all the excitations, are gathered in order to carry on our study. The conclusion from the NI is important to fill up the matrix with the best (more excited) rigid modes (relative to the nine measured directions). With such a matrix, relative to the nine measured directions with the most excited mode shapes, we proceed to the necessary coordinate transformation (Eq. (4)) to obtain the rigid body modes matrix relative to the defined origin.

For both suspension conditions A and B, the rigid body modal matrix is constructed (relative to the nine measured directions) with the following information:

$$\bullet\text{Set 1}\begin{cases} F_{0_x}(\text{set-upA}) - \{\text{1st mode} \\ F_{0_y}(\text{set-upA}) - \begin{cases}\text{3rd mode}\\ \text{5th mode}\\ \text{6th mode}\end{cases} \\ F_{0_z}(\text{set-upA}) - \begin{cases}\text{2nd mode}\\ \text{4th mode}\end{cases}\end{cases} \cdot \text{Set 2}\begin{cases} F_{1x}(\text{set-upB}) - \begin{cases}\text{1st mode}\\ \text{4th mode}\end{cases} \\ F_{2y}(\text{set-upB}) - \begin{cases}\text{2nd mode}\\ \text{3rd mode}\\ \text{5th mode}\\ \text{6th mode}\end{cases}\end{cases}.$$

Figs. 5–7 show the results that are obtained using the modal method developed by Bretl and Conti and the method proposed by Toivola and Nuutila. The results of the application of force F_{2y} in set-up B, for the inertia

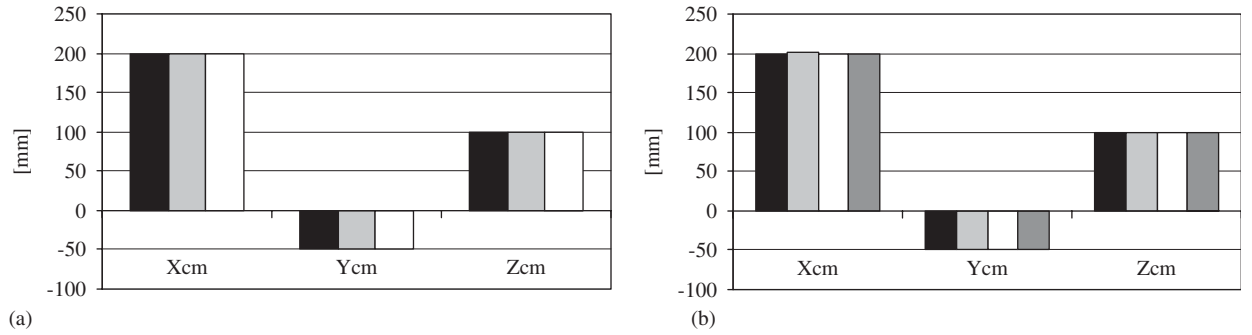

Fig. 6. Results of the centre of mass coordinates for (a) sets 1 and 2 using Bretl and Conti method and (b) for sets 1, 2 and F_{2_y} with Toivola and Nuutila method. ■, correct; ▒, F_{2_y}; □, set 1; ▒, set 2.

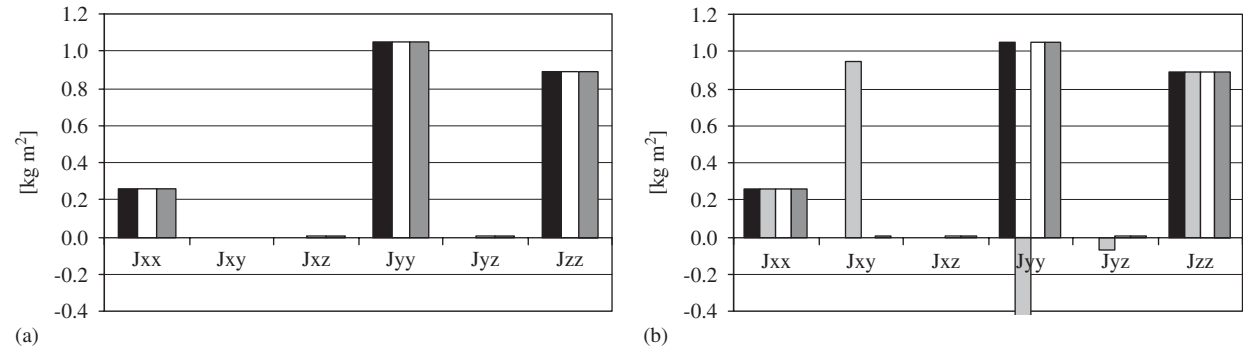

Fig. 7. Results of the inertia tensor parameters for (a) sets 1 and 2 using Bretl and Conti method and (b) for sets 1, 2 and F_{2_y} with Toivola and Nuutila method. ■, correct; ▒, F_{2_y}; □, set 1; ▒, set 2.

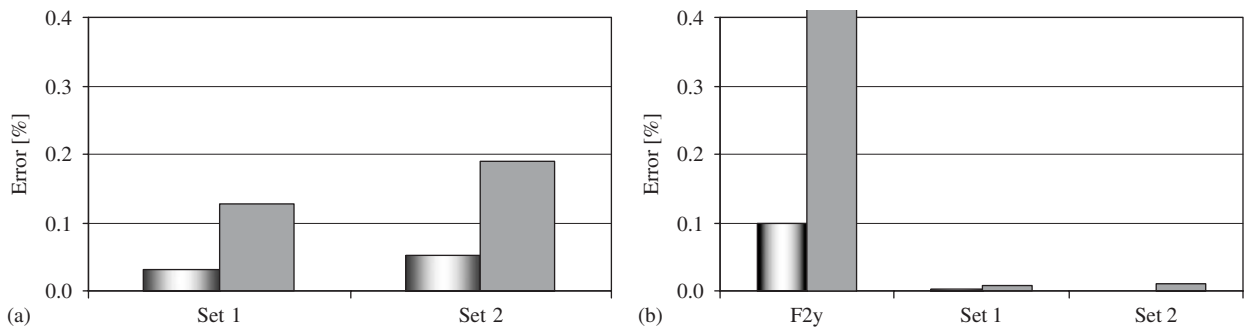

Fig. 8. Results of the relative error of the vectors of the centre of mass coordinates and inertia parameters for (a) sets 1 and 2 using Bretl and Conti method and (b) for sets 1, 2 and F_{2_y} using Toivola and Nuutila method. ▒, $\mathbf{C}_{cm}$; ▒, $\mathbf{J}_{cm}$.

parameters with sets 1 and 2, are obtained using only Toivola and Nuutila method, as the former method requires the identification of all the six rigid body modes. Fig. 5 also shows the relative error remaining on the mass parameter (m) of the rigid body. Fig. 8 shows the relative error obtained on the vector of the centre of mass coordinates $\mathbf{C}_{cm} = \{x_{cm} \quad y_{cm} \quad z_{cm}\}$ and on the vector of moments and inertia products $\mathbf{J}_{cm} = \{J_{xx} \quad J_{xy} \quad J_{xz} \quad J_{yy} \quad J_{yz} \quad J_{zz}\}$.

3.1.1. Remarks

1. From the observation of these results, first a conclusion can be extracted: with the use of the information from rigid body modes excited by different forces, it became possible to determine accurate rigid body

properties; this would have been impossible if the new approach tool had not been used, because none of the applied forces excite all the six rigid body modes. However, the Toivola and Nuutila method provides better results than the Bretl and Conti method, as shown in the corresponding graphics of the calculated error on vectors $\mathbf{C}_{cm}$ and $\mathbf{J}_{cm}$.

2. On the other hand, from the results obtained with the excitation force in set-up B, one can conclude that the Toivola and Nuutila method allows for the determination of the majority of the parameters with small error percentage. The most critical parameter is the inertia moment J_{yy} and inertia products J_{xy}, J_{yz} as they require the information about the non-excited rigid body modes related to the θ_y rotation.

3.2. Test Case II—experimental

An experimental case study is based on the test article presented in Fig. 9. The measurement points have been selected and three excitation forces have been applied via an impact hammer with a rubber tip (BK 8202). Once again, the measurement points were selected taking into due account the recommendations proposed by Lee et al. [20]. Flexible springs with low mass have been used to suspend the rigid body. A triaxial accelerometer (BK 4506 B) was used for the measurements. The FRFs have been measured and processed by a four channel BK 2035 analyser, allowing for the simultaneous acquisition of the three responses and one force, in the range 0–12.5 Hz.

The inertia parameters of the experimental test case have been obtained using the SolidWorks software; these values are here assumed as the reference values for the sake of comparison:

Mass = 15.69 kg

Centre of mass coordinates relative to each origin: (mm)

Origin I	Origin II	Origin III
$x_{g_1} = 177.25$	$x_{g_2} = 75.45$	$x_{g_3} = 39.15$
$y_{g_1} = 30.40$	$y_{g_2} = -184.42$	$y_{g_3} = 86.08$
$z_{g_1} = -5.35$	$z_{g_2} = -61.069$	$z_{g_3} = 127.43$

Inertia moments relatiely to the centre of mass cocordiantes: (kg m^2)

$J_{xx} = 0.35733194$	$J_{xy} = 0.07722671$	$J_{xz} = -0.08736156$
$J_{yx} = 0.07722671$	$J_{yy} = 0.39469014$	$J_{yz} = -0.06919817$
$J_{zx} = -0.08736156$	$J_{zy} = -0.06919817$	$J_{zz} = 0.31706832$

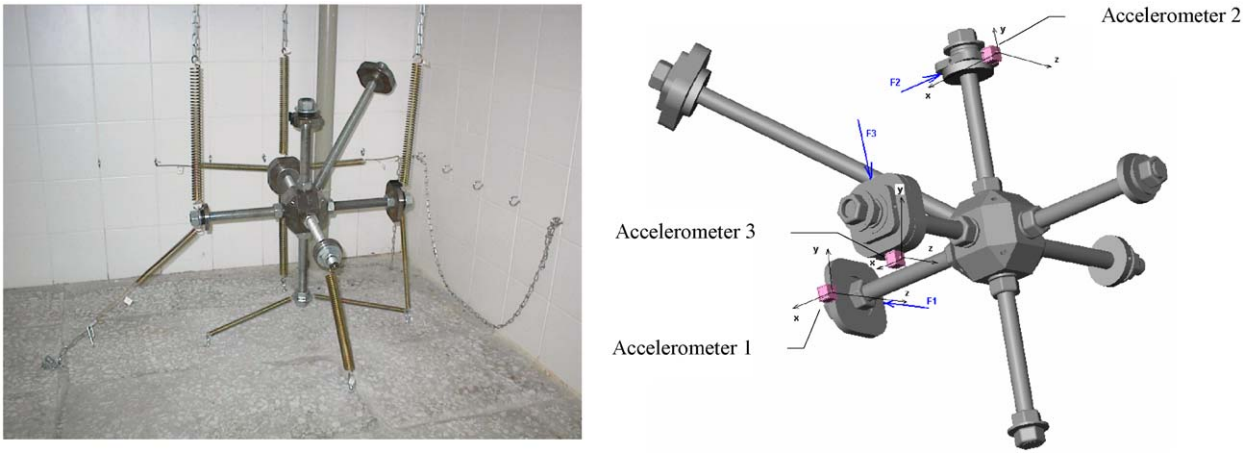

Fig. 9. Rigid body studied in the experimental test case.

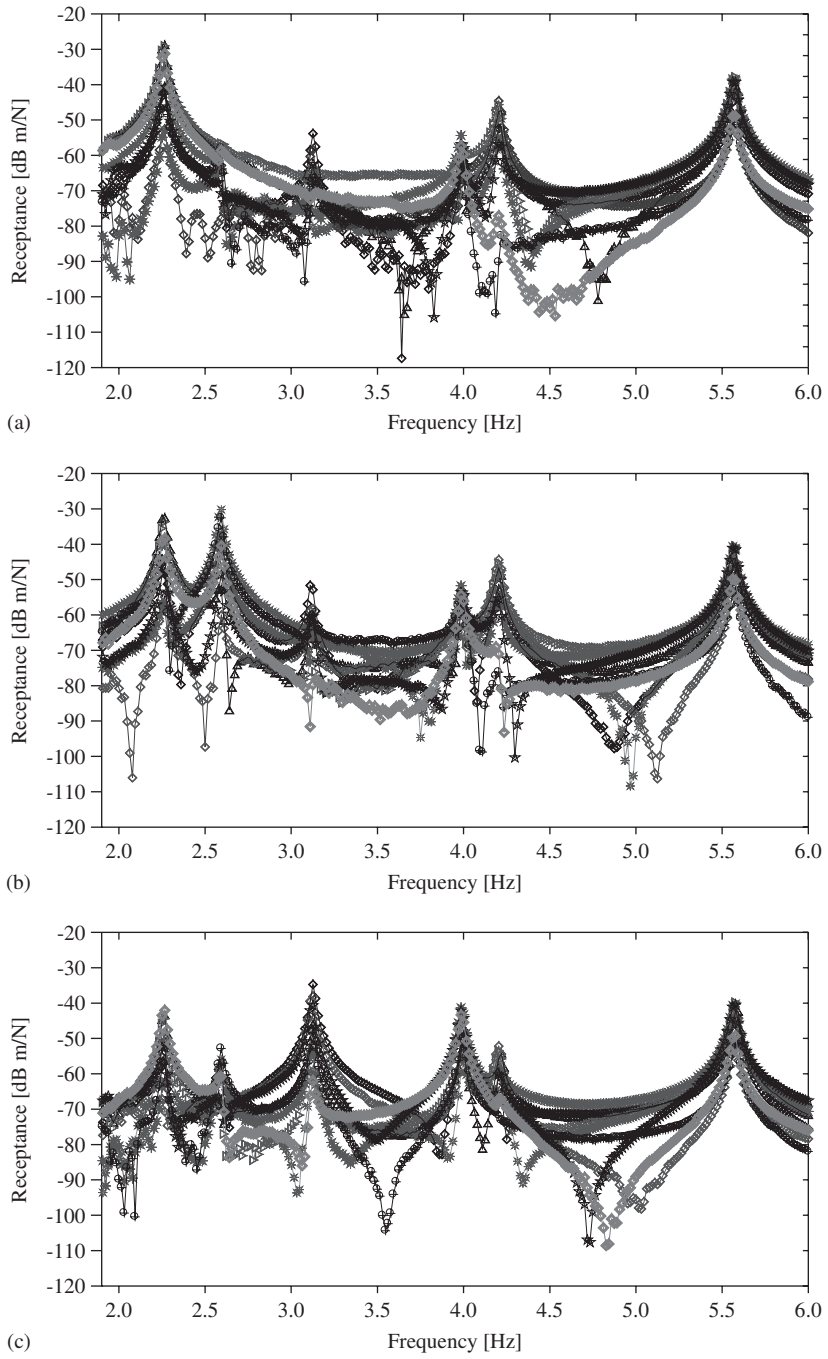

Fig. 10. Receptance FRFs for each applied forces in the experimental test case; (a) force 1, (b) force 2, (c) force 3. —⊕—, x_1; —◇—, y_1; —△—, z_1; —✳—, x_2; —△—, y_2; —▷—, z_2; —✶—, x_3; —☆—, y_3; —◇—, z_3.

At a second stage a SIMO modal analysis was performed using MODENT [31] for the identification of the modal parameters. Fig. 10 represents all of the nine FRFs obtained for each excitation force.

In Fig. 11 the results obtained with the NI for all the applied forces are presented.

Using the NI [29,30], one expects that the results can be improved by using not only information about the rigid body modes obtained from only one excitation force, but also the information available from the different set of modes gathered for several forces, such as demonstrated in test case I.

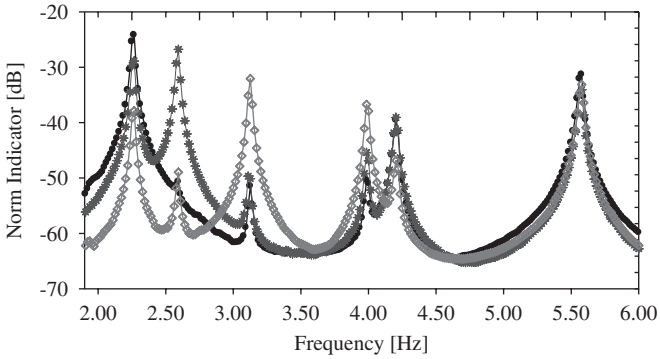

Fig. 11. Norm Indicator results for the experimental test case with applied forces. —●—, force 1; —✳—, force 2; —◇—, force 3.

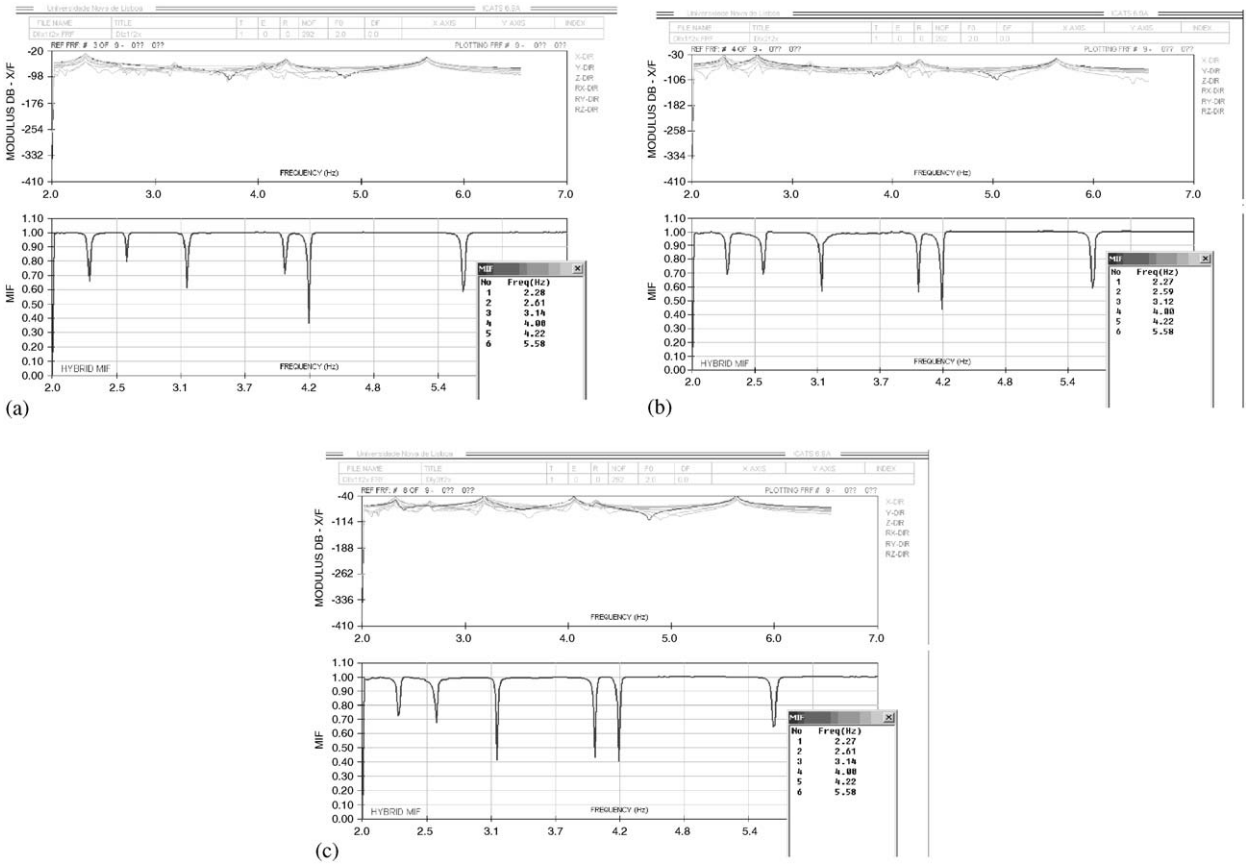

Fig. 12. Hybrid MIF results for each applied force in the experimental test case: (a) force 1, (b) force 2, (c) force 3.

In order to assess the performance of the NI and also to help us choosing which rigid body modes should be selected for each force (to construct the matrix of all rigid modes related to the nine measured directions) it was decided to use two other Mode Indicator Functions (MIF) together with the NI. These MIFs are calculated for each excitation force with the information of the nine FRFs measured with the three triaxial accelerometers:

1. NI [29,30].
2. Hybrid MIF [32]—estimate MIF of all FRFs measured with three triaxial accelerometers, using both real and imaginary parts of the FRFs.
3. PRF MIF—developed by Rades and Ewins [33,34].

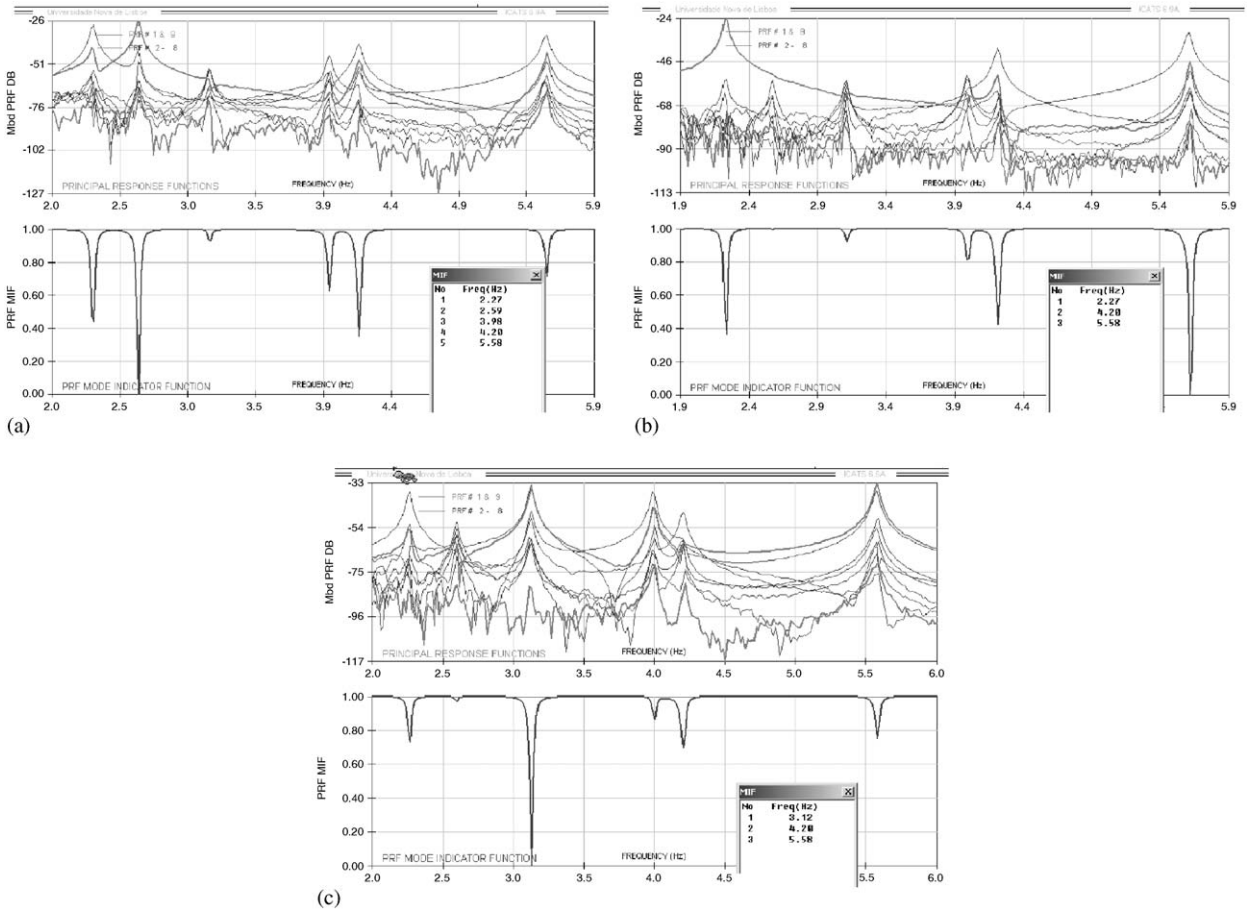

Fig. 13. PRF MIF results for each applied force in the experimental test case: (a) force 1, (b) force 2, (c) force 3.

The graphics referring to the application of the hybrid MIF and PRF MIF to the nine FRFs are presented in Figs. 12 and 13, respectively.

With that information it was decided to define five sets combining all the information, three of them based on MIFs information, and the remaining two defined with no particular criterion:

$$\text{Set I (No criterion)}\begin{cases}\text{1st mode} - \text{force 2}\\ \text{2nd mode} - \text{force 2}\\ \text{3rd mode} - \text{force 3}\\ \text{4th mode} - \text{force 3}\\ \text{5th mode} - \text{force 1}\\ \text{6th mode} - \text{force 1}\end{cases}, \quad \text{Set II (PRF-MIF)}\begin{cases}\text{1st mode} - \text{force 1}\\ \text{2nd mode} - \text{force 2}\\ \text{3rd mode} - \text{force 3}\\ \text{4th mode} - \text{force 2}\\ \text{5th mode} - \text{force 2}\\ \text{6th mode} - \text{force 1}\end{cases},$$

$$\text{Set III (NI)}\begin{cases}\text{1st mode} - \text{force 1}\\ \text{2nd mode} - \text{force 2}\\ \text{3rd mode} - \text{force 3}\\ \text{4th mode} - \text{force 3}\\ \text{5th mode} - \text{force 2}\\ \text{6th mode} - \text{force 1}\end{cases}, \quad \text{Set IV (No criterion)}\begin{cases}\text{1st mode} - \text{force 1}\\ \text{2nd mode} - \text{force 2}\\ \text{3rd mode} - \text{force 3}\\ \text{4th mode} - \text{force 3}\\ \text{5th mode} - \text{force 1}\\ \text{6th mode} - \text{force 3}\end{cases},$$

$$\text{Set V (Hybrid-MIF)}\begin{cases}\text{1st mode} - \text{force 1}\\ \text{2nd mode} - \text{force 3}\\ \text{3rd mode} - \text{force 3}\\ \text{4th mode} - \text{force 3}\\ \text{5th mode} - \text{force 1}\\ \text{6th mode} - \text{force 1}\end{cases}.$$

The modal matrix, relative to the nine measured directions is constructed with the information of the most excited mode shapes, for sets II, III and V, which can be observed in Figs. 11–13, respectively.

Following the definition of each set, it is necessary to check their performance comparatively to three assumed coordinate origins. The three predefined coordinate origins correspond to the position of the three triaxial accelerometers. The distance between each origin and the centre of mass, $\vec{d}_{i\to\mathrm{cm}}$, is

- Origin I—accelerometer 1, $\vec{d}_{1\to\mathrm{cm}} = 207.1\,\mathrm{mm}$;
- Origin II—accelerometer 2, $\vec{d}_{2\to\mathrm{cm}} = 208.4\,\mathrm{mm}$;
- Origin III—accelerometer 3, $\vec{d}_{3\to\mathrm{cm}} = 158.7\,\mathrm{mm}$.

The relative errors for the mass value, the vector position of centre of mass $\mathbf{C}_{\mathrm{cm}}$ and the vector of moments and products of inertia $\mathbf{J}_{\mathrm{cm}}$, for each data set and for each considered origin are presented, respectively in Figs. 14–16.

If all the parameters errors are added, the following equation is obtained: $\sum \mathrm{Errors} = \sum(\mathrm{Error}(m) + \mathrm{Error}(\mathbf{C}_{\mathrm{cm}}) + \mathrm{Error}(\mathbf{J}_{\mathrm{cm}}))$. The results are presented in Fig. 17.

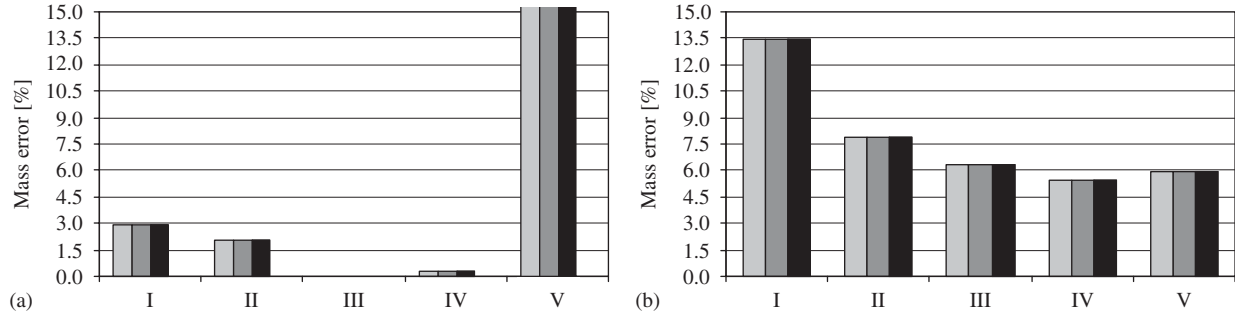

Fig. 14. Level of error of the mass parameter, for various sets and origins using (a) Bretl and Conti method and (b) Toivola and Nuutila method. □, Origin I; ▒, Origin II; ■, Origin III.

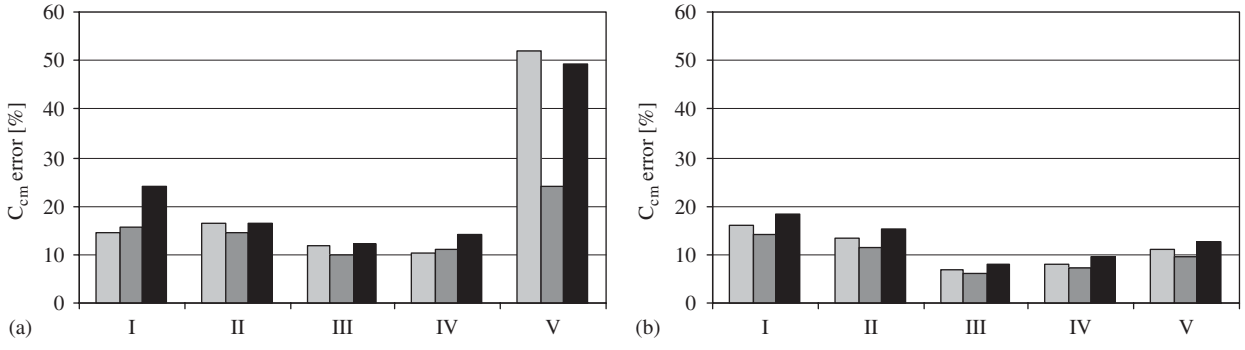

Fig. 15. Level of error of the centre of mass coordinates, for various sets and origins using, (a) Bretl and Conti method, (b) Toivola and Nuutila method. □ Origin I, ▒ Origin II, ■ Origin III.

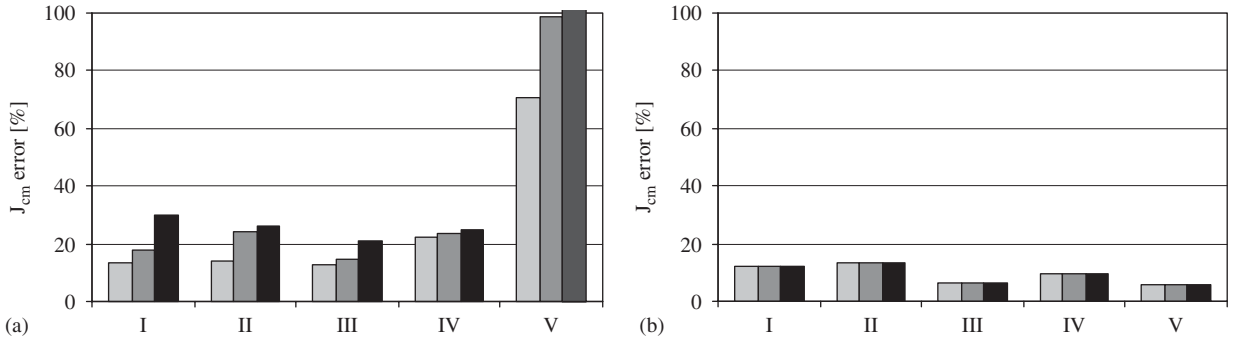

Fig. 16. Level of error of the inertia tensor parameters, for various sets and origins using (a) Bretl and Conti method and (b) Toivola and Nuutila method. □, Origin I; ▒, Origin II; ■, Origin III.

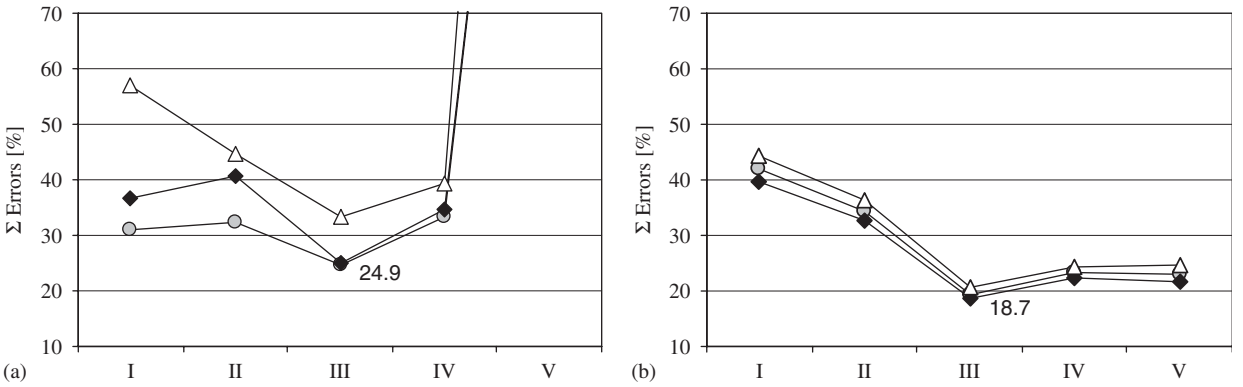

Fig. 17. Summation of all the parameters errors for the various sets and origins (a) Bretl and Conti method and (b) Toivola and Nuutila method. —○—, Origin I; —◆—, Origin II; —△—, Origin III.

4. Conclusions

From the present study some important conclusions can be drawn:

1. The quality of the obtained results for the inertia parameters with both Bretl and Conti and Toivola and Nuutila methods is highly dependent on the quality and quantity of the identified rigid body modes.
2. The main restriction for the use of Bretl and Conti method is associated to the number of excited rigid body modes. In fact this method cannot be used when not all the rigid body modes are excited or a double mode exists. In contrast, Toivola and Nuutila method does not have this problem for the determination of the ten unknowns, since it requires at least four identified mode shapes. However, the results improve as soon as six rigid body modes are used (see case I for force F_{2y}—Figs. 5 and 8).
3. Another conclusion is that better results can be obtained if one uses the information of the rigid body modes extracted from the FRFs resulting from several forces. In fact, the best modes can be selected by using the concept of NI, which can reveal a particular set in the present study (set III—experimental case). This indicator shows (i), for any applied force(s) and in the frequency range of interest, how many rigid modes exist and (ii) for a set of applied forces, which are the most excited modes. This characteristic is not revealed in the other two indicators that have been used (Hybrid MIF and PRF MIF—Figs. 12 and 13) (see results obtained with sets II, III, V, for experimental case—Figs. 14–17). The importance of the use of this NI is illustrated with the results obtained for sets II and III. In fact, the only difference resides on the choice of the fourth rigid body mode to construct the modal matrix; in the first set it was selected the one obtained from force 2, whereas in the second set it was selected the one from force 3.

4. The parameters referring to the centre of mass coordinates and inertia tensor are better obtained with Toivola and Nuutila method rather than with Bretl and Conti method. This is not always the case for the mass value (see Figs. 5 and 14). However, this aspect is not so critical, as the mass property can be evaluated with alternative simple methods.
5. Observing the results obtained for the errors on the centre of mass coordinates with Toivola and Nuutila method, it can be verified that there exists a relation between these results and the distance between the origin of the referential coordinates and the centre of mass of the rigid body. As it can be seen in Fig. 15, the results improve as the distance increases.
6. The results presented in Fig. 14 also show that in both methods the relative error in the rigid body mass is invariant with respect to the chosen origin. The same conclusion is true for the relative error of $\mathbf{J}_{cm}$ in Toivola and Nuutila method, Fig. 16.

References

[1] Y.S. Wei, J. Reis, Experimental determination of rigid body inertia properties, in: Proceedings of the Seventh International Modal Analysis Conference, Las Vegas, NV, 1989, pp. 603–606.
[2] A. Fregolent, A. Sestieri, M. Falzetti, Identification of rigid body inertia properties from experimental frequency response, in: Proceedings of the 10th International Modal Analysis Conference, San Diego, CA, 1992, pp. 219–225.
[3] J.A. Mangus, Estimating rigid body properties from force reaction measurements, in: Proceedings of the 11th International Modal Analysis Conference, Kissimmee, FL, 1993, pp. 469–472.
[4] C. Schedlinski, M. Link, On the identification of rigid body properties of an elastic system, in: Proceedings of the 15th International Modal Analysis Conference, Orlando, FL, 1997, pp. 1588–1594.
[5] C. Schedlinski, M. Link, A survey of current inertia parameter identification methods, *Mechanical Systems and Signal Processing* 15 (1) (2001) 189–211.
[6] F. Holzweissig, H. Dresig, *Lehrbuch der Maschinendynamic: Grundlagen und Praxisorientierte Beispiele, mit 40 Aufgaben mit Lösungen und 53 Talellen*, Fachbuchverlag neubearb, Aufl Leipzig, Köln, 1994.
[7] S.M. Pandit, Z.-Q. Hu, Determination of rigid body characteristics from time domain modal test data, *Journal of Sound and Vibration* 177 (1) (1994) 31–41.
[8] H. Hahn, Inertia parameter identification of rigid bodies using a multi-axis test facility, in: Proceedings of the Third IEEE Conference on Control Applications, Glasgow, 1994, pp. 1735–1737.
[9] D.J. Ewins, *Modal Testing: Theory and Practice*, Research Studies Press Ltd., Somerset, England, 1995.
[10] M.A. Lamontia, On the determination and use of residual flexibilities, inertia restraints and rigid body modes, in: Proceedings of the First International Modal Analysis Conference, Orlando, FL, 1982, pp. 153–159.
[11] J. Crowley, T. Rocklin, D. Brown, Use of rigid body calculations in tests, in: Proceedings of the Fourth International Modal Analysis Conference, Los Angeles, CA, 1986, pp. 487–493.
[12] M. Furusawa, T. Tominaga, Rigid body modes enhancement and RDOF estimation for experimental modal analysis, in: Proceedings of the Fourth International Modal Analysis Conference, Los Angeles, CA, 1986, pp. 1149–1155.
[13] N. Okubo, T. Furukawa, Measurement of rigid body modes for dynamic design, in: Proceedings of the Second International Modal Analysis Conference, 1983, pp. 545–549.
[14] Y.S. Wei, J. Reis, Experimental determination of rigid body inertia properties, in: Proceedings of the Seventh International Modal Analysis Conference, Las Vegas, NV, 1989, pp. 603–606.
[15] M. Furukawa, A method of determining of rigid body inertia properties, in: Proceedings of the Seventh International Modal Analysis Conference, Las Vegas, NV, 1989, pp. 711–719.
[16] H. Okuzumi, Identification of rigid body inertia characteristics of a power plant by using experimentally obtained transfer functions, JSAE Review 1991, *Society of Automotive Engineering of Japan, no. 12* (1991) 28–32.
[17] J. Bretl, P. Conti, Rigid body mass properties from test data, in: Proceedings of the Fifth International Modal Analysis Conference, London, England, 1987, pp. 655–659.
[18] A. Fregolent, A. Sestieri, M. Falzetti, Identification of rigid body inertia properties from experimental frequency response, in: Proceedings of the 10th International Modal Analysis Conference, San Diego, CA, 1992, pp. 219–225.
[19] A. Fregolent, A. Sestieri, Identification of rigid body inertia properties from experimental data, *Mechanical Systems and Signal Processing* 10 (6) (1996) 697–709.
[20] H. Lee, Y. Park, Y. Lee, Response and excitation points selection for accurate rigid body inertia properties identification, *Mechanical Systems and Signal Processing* 1 (4) (1999) 571–592.
[21] A. Urgueira, R. Almeida, Dynamic properties of rigid Body systems from vibration measurement, in: Proceedings of the International Conference on Structural Dynamics Modelling, Portugal, Madeira, 2002, pp. 211–215.
[22] C. Johnson, V. Snyder, Using complex frequency response functions to determine system matrices of vibratory systems, in: Proceedings of the Sixth International Modal Analysis Conference, Kissimmee, FL, 1988, pp. 701–704.
[23] J.A. Mangus, C. Passarelo, C. Vankarsen, Direct estimation of rigid body properties from frequency response functions, in: Proceedings of the 10th International Modal Analysis Conference, San Diego, CA, 1992, pp. 259–264.

[24] S.J. Huang, S. Cogan, G. Lallement, Experimental identification of the characteristics of a rigid structure on an elastic suspension, in: Proceedings of the 13th International Modal Analysis Conference, Nashville, TN, 1995, pp. 955–961.
[25] S.J. Huang, G. Lallement, Direct estimation of rigid body properties from harmonic forced responses, in: Proceedings of the 15th International Modal Analysis Conference, Orlando, FL, 1997, pp. 175–180.
[26] P. Conti, J. Bretl, Mount stiffnesses and inertia properties from modal test data, *Journal of Vibration, Acoustics, Stress and Reability in Design* 111 (1989) 134–138.
[27] J. Toivola, O. Nuutila, Comparison of three methods for determining rigid body inertia properties from frequency response functions, in: Proceedings of the 11th International Modal Analysis Conference, Kissimmee, FL, 1997, pp. 1126–1132.
[28] N. Maia, J. Silva, J. He, N. Lieven, R. Lin, G. Skingle, W. To, A. Urgueira, *Theoretical and Experimental Modal Analysis*, Research Studies Press, Taunton, Somerset, UK, 1997.
[29] R. Almeida, Determinação de Características Dinâmicas de Corpos Rígidos com Base em Resultados Experimentais, Ph.D. Thesis, Faculdade de Ciências e Tecnologia da Universidade Nova de Lisboa, 2004.
[30] R. Almeida, A.P.V. Urgueira, N.M.M. Maia, Evaluation of rigid body properties from frequency response data, in: Proceedings of the International Conference on Modal Analysis Noise and Vibration Engineering, Leuven, Belgium, 2004, pp. 2409–2423.
[31] MODENT, Integrated Software for Structural Dynamic, ICATS 1988–2000, Imperial College of Science, Technology and Medicine, University of London, UK.
[32] M. Rades, A comparison of some mode indicator functions, *Mechanical Systems and Signal Processing* 8 (4) (1994) 459–474.
[33] M. Rades, D.J. Ewins, The aggregate mode indicator function, in: Proceedings of the 18th International Modal Analysis Conference, San Antonio, TX, 2000, pp. 201–207.
[34] M. Rades, D.J. Ewins, Principal response analysis in structural dynamics, in: Integrated Software for Structural Dynamics, 〈http://www.icats.co.uk/pubs/principal.pdf〉, ICATS Selected Papers.